

OBSERVATIONS OF A BIMODAL SIZE DISTRIBUTION FOR THE AEROSOL PARTICLES ON MARS BY SPICAM/MEX

A. Fedorova, A. Rodin, O. Korablev, IKI (Space Research Institute), Moscow, Russia; Moscow Institute of Physics and Technology (MIPT), 9 Institutsky dr., 141700 Dolgoprudny, Moscow Region, Russia (fedorova@iki.rssi.ru), F. Montmessin, A. Määttä, J.-L. Bertaux, CNRS LATMOS, 11 Bd d'Alembert, 78280 Guyancourt, France, L. Maltagliati, LESIA, Observatoire Paris-Meudon, 4 place Jules Janssen, France

Introduction:

Dust aerosols play an important role in the Martian climate system. The spatial and temporal variability and optical properties of atmospheric aerosols has been a target of almost every major spacecraft mission to Mars. Airborne dust is composed mostly of mineral particles lifted from the surface by near-surface winds and presumably by “dust devils”, small-scale convective vortex. Dust participates in heating and cooling of different atmospheric layers absorbing, scattering and reemitting in thermal IR solar radiation [1, 2]. Aerosol particles serve also as cloud condensation nuclei (CCN) in the Martian atmosphere and thus help regulate the transfer of water between the hemispheres [3].

Since condensate clouds were observed in Martian atmosphere, besides the main micron-size mode extended microphysical modeling requires a small dust particle population in the higher region of the atmosphere in order to form a clouds agreeing with data. Some observations supported the bimodal distribution against the mono-modal mostly used to characterize the Martian dust. Based on Viking limb radiance observations and microphysical modeling, Montmessin et al. (2002) [4] have derived a bimodal distribution at $L_s=176^\circ / 15^\circ\text{S}$ (shortly before the dust storm), featuring two maxima with $r_{\text{eff}}=1.8 \mu\text{m}$ and $v_{\text{eff}}=0.5 \mu\text{m}$ for the large mode and $<0.2 \mu\text{m}$ for the small mode, with a ratio of populations (small to large) around 25. Markiewicz et al. (1999) have reported a possible presence of bimodal distribution based on the Imager for Mars Pathfinder (IMP) data on the midday sky brightness in visible-near-IR filters at $L_s \sim 156^\circ$ [5].

Data analysis: The spectral range of SPICAM IR (1-1.7 μm) includes three relatively strong CO_2 absorption bands (1.43, 1.57 and 1.6 μm) and the 1.37- μm H_2O band [6]. To reduce the number of spectral sampling points in solar occultation, the IR spectrum consists of three “windows” and a set of several continuum points [see 6-7 for details]. We used the set of 10 continuum wavelengths outside gaseous absorption bands: 996.4, 1093.7, 1158.2, 1197.0, 1241.4, 1272.9, 1304.4, 1321.9, 1514.6 and 1552.2 nm.

The UV spectrometer measures a spectrum from 118 to 310 nm and includes the absorption bands of CO_2 , O_3 and continuum extinction by aerosols. The retrieval method separates the various species in a way described in [8-9]. For the present study, aerosol extinctions at wavelengths of 200, 250 and 300 nm have been used.

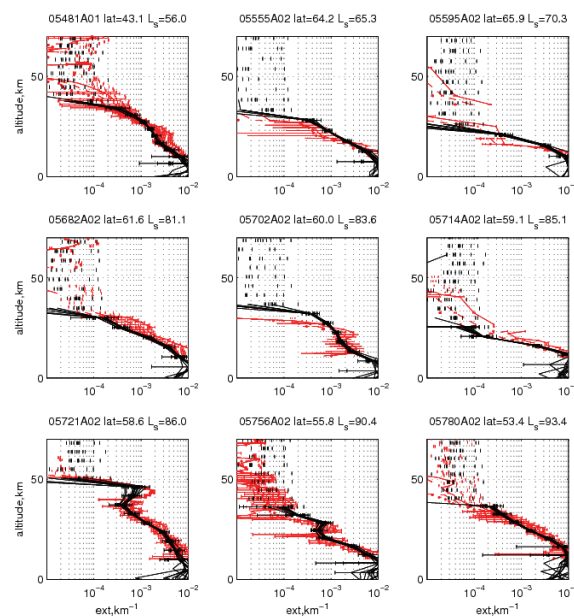


Figure 1. The IR and UV extinctions for the Northern hemisphere. Black lines are the IR extinctions for 12 wavelengths, and red lines are the UV extinctions for three wavelengths.

The hypothesis of a bimodal size distribution for Martian dust, the main motivation of this work, has been tested against observations chosen at the beginning of summer in the northern hemisphere in MY29 ($L_s=56-97^\circ$). This season is especially interesting due to the recent detection of supersaturation of water vapour that was previously discussed for its link to the size and nature of dust condensation nuclei [10]. The series of observations consists of 9 profiles in the northern hemisphere (fig.1) and 11 at the southern hemisphere (fig.2) at latitudes of 40-65°N and 30-62°S respectively. The latitudes cover cold dust-clear area near the polar night in the southern hemisphere and the middle and high northern latitudes corresponding to the edge of aphelion cloud

belt and the range free of clouds at 60°N.

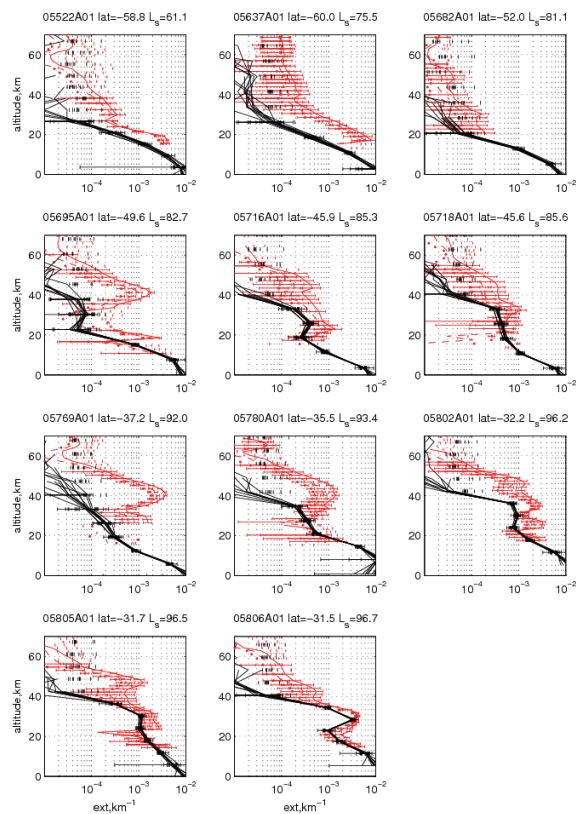


Figure 2. The IR and UV extinctions for the Southern hemisphere.

The interpretation of the profiles using Mie scattering theory with adequate refractive indices of Martian dust and H₂O ice particles allows to retrieve a particle size distribution and number density [7]. Figures 3 and 4 present vertical distributions of particle size for dust, ice and small mode and number density profiles for 5 orbits in the Northern hemisphere for latitudes >60°N, L_s=65-85° and for 3 orbits in the Southern hemisphere for latitudes >50°S, L_s=61-81° as examples.

Summary: For the first time, a combined analysis of the UV and IR channels in the spectral range from 200 to 1550 nm has allowed to derive unambiguously a bimodal size distribution for Martian aerosols in an altitude range of 10-70 km and to track its vertical and temporal evolution:

1) The main mode of the distribution has been determined both for H₂O and dust particles with a retrieved average radius of 0.7 and 1.3 μm, respectively. We are unable to separate ice and dust from SPICAM observations, so we based our interpretation on MCS observations for the same season and MY29 [11]

2) A small mode of submicron particles has been detected for both hemispheres. The average radius is 0.044 μm and number density varies from 2 cm⁻³ at 60 km to 10⁴ cm⁻³ at 20 km for the Northern hemisphere.

The average radius is 0.066 μm and the number density ranges from 1 cm⁻³ at 60 km to 10³ cm⁻³ at 20 km for the southern hemisphere. The small mode extends vertically up to 70 km in the Southern hemisphere whereas it remains around 30-40 km in the Northern hemisphere.

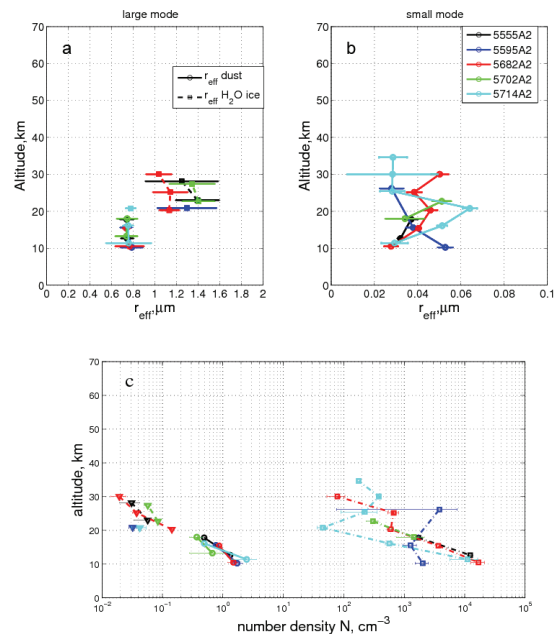


Figure 3. Retrieved profiles of particle size and number density for the two modes of the bimodal distribution, assuming dust or ice refractive index. The results for five orbits in the Northern hemisphere for latitudes >60°N are presented.

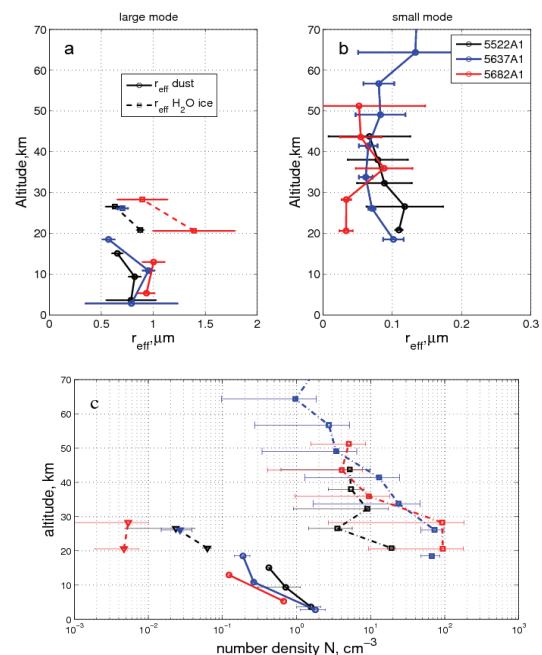


Figure 4. Same as in Fig. 3 for three orbits in the Southern hemisphere for latitudes >50°S.

3) Low-altitude clouds have been observed at 20-30 km. Such clouds correspond to the poleward edge of the aphelion cloud belt both in the Southern

and the Northern hemisphere. Their opacity in UV and IR is below 0.03.

4) Clouds in the Southern hemisphere have been detected at 40-50 km in the UV only with a total opacity below 0.05, too small to be detected in nadir (sub-visible clouds). The average particle size is $\sim 0.06 \mu\text{m}$ and the number density in the clouds varies from 100 to 5000 cm^{-3} .

5) The highest level of supersaturation at the Northern hemisphere at altitudes of 30-50 km reported in [10] for latitudes $> 60^\circ\text{N}$ is consistent with the observed absence of any particles (small or large) above 30 km in our observations. For latitudes below 60°N it is more difficult to explain the supersaturation since at least $10\text{-}100 \text{ cm}^{-3}$ particles has been observed at 30-50 km with $r_{\text{eff}} \approx 0.05 \mu\text{m}$ on average. Our estimation of the critical saturation ratio based on the nucleation rate calculation gives $S_{\text{crit}} \sim 2$ for particles from 0.01 to $0.1 \mu\text{m}$. The high supersaturation may be explained by high values of S_{crit} at low temperatures reported by several authors [12]. In the Southern hemisphere the small particles with $r \sim 0.07 \mu\text{m}$ are always present but $S_{\text{crit}} < 4$ derived by Maltagliati et al. (2011) [10] is within the uncertainties of nucleation rate and temperature dependence.

6) Brownian coagulation quickly removes particles with $r < 0.1 \mu\text{m}$ and number density $\geq 1000 \text{ cm}^{-3}$. For the small mode with $r_{\text{eff}} = 0.04\text{-}0.05 \mu\text{m}$ and $N \sim 10^3 \text{ cm}^{-3}$ in the Northern hemisphere a source of particles is required to balance the loss by coagulation. Micrometeorite mass flow estimations are too low, whereas a surface source (wind stress dust lifting and dust devils) appears more plausible. In the Southern hemisphere the small mode with $r_{\text{eff}} = 0.07 \mu\text{m}$ and $N < 10^2 \text{ cm}^{-3}$ is more stable and can survive 50-100 days or more. Similar to the Earth aerosol distribution, coagulation of small particles could explain the bimodal type of distribution.

The Mars Express occultation database is large and is being continuously populated [9, 10]. Further analysis of the IR and UV solar occultations would help to constrain the seasonal and geographical variations of the small and large modes of aerosols. Considering the impact of aerosols on present-day Mars climate, the present study opens a new path of exploration for modelers in their research.

Acknowledge: We thank our collaborators at the three institutes for the design and the fabrication of the instruments (Service d'Aeronomie/France, BIRA/Belgium and IKI/Moscow). AF, OK and AR acknowledge the program 22 of RAS and the Russian Government grant to the Moscow Institute of Physics and Technology № 11.G34.31.0074 for finance support.

References:

[1] Medvedev A.S., Kuroda T. and Hartogh P.: Influence

of dust on the dynamics of the martian atmosphere above the first scale height, *Aeolian Research*, Vol. 3, pp. 145-156, 2011.

[2] Madeleine J.-B., Forget F., Millour E., Montabone L., and M. J. Wolff: Revisiting the radiative impact of dust on Mars using the LMD Global Climate Model, *J. Geophys. Res.*, Vol. 116, E11010, doi:10.1029/2011JE003855, 2011.

[3] Montmessin, F., Forget, F., Rannou, P., Cabane, M., Haberle, R.M.: Origin and role of water ice clouds in the Martian water cycle as inferred from a general circulation model. *J. Geophys. Res.(E)*, Vol. 105, pp. 4109-4121, 2004.

[4] Montmessin, F., Rannou, P. and Cabane, M.: New insights into Martian dust distribution and water-ice cloud microphysics. *J. Geophys. Res.*, Vol. 107 (E6), pp. 4-1, CiteID 5037, DOI 10.1029/2001JE001520, 2002.

[5] Markiewicz, W.J., Sablotny, R.M., Keller, H.U., Thomas, N., Titov, D., Smith, P.H. 1999. Optical properties of the Martian aerosols as derived from Imager for Mars Pathfinder midday sky brightness data. *J. Geophys. Res.* 104 (E4), 9009-9018.

[6] Korabiev O. et al.: SPICAM IR acousto-optic spectrometer experiment on Mars Express. *J. Geophys. Res.*, Vol. 111, E09S03, doi:10.1029/2006JE002696, 2006.

[7] Fedorova A. et al.: Solar Infrared Occultations by the Spicam Experiment on Mars-Express: Simultaneous Observations of H_2O , CO_2 and Aerosol Vertical Distribution, *Icarus*, Vol. 200, Is. 1, pp. 96-117, doi:10.1016/j.icarus.2008.11.006, 2009.

[8] Montmessin F. et al.: Stellar Occultations at UV wavelengths by the SPICAM instrument: retrieval and analysis of Martian haze profiles, *J. Geophys. Res.*, Vol. 111, E09S09, doi: 10.1029/2005JE002662, 2006.

[9] Määttänen A. et al.: A complete climatology of the aerosol vertical distribution on Mars from MEx/SPICAM UV solar occultations, *Icarus*, Vol. 223, pp. 892-941, 2013.

[10] Maltagliati L. et al.: Evidence of water vapor in excess of saturation in the atmosphere of Mars, *Science*, Vol. 333, pp. 1868-1871, 2011.

[11] McCleese D.J., et al.: Structure and dynamics of the Martian lower and middle atmosphere as observed by the Mars Climate Sounder: Seasonal variations in zonal mean temperature, dust, and water ice aerosols, *J. Geophys. Res.*, Vol. 115, E12, E12016, doi: 10.1029/2010JE003677, 2010.

[12] Ladino L.A., Abbatt J.P.D.: Laboratory investigation of Martian water ice cloud formation using dust aerosol stimulants, *J. Geophys. Res.*, Vol. 118, pp. 1-12, doi:10.1029/2012JE004238, 2013.

[13] Maltagliati, L. et al.: Annual survey of water vapor vertical distribution and water-aerosol coupling in the martian atmosphere observed by SPICAM/MEx solar occultations, *Icarus*, Vol. 223, Is. 2, pp. 942-962, 2013.